

## High-Frequency Stress Relaxation in Semiflexible Polymer Solutions and Networks

G. H. Koenderink,\* M. Atakhorrami, F. C. MacKintosh, and C. F. Schmidt†

*Department of Physics and Astronomy, Vrije Universiteit, Amsterdam, The Netherlands*

(Received 15 July 2005; published 7 April 2006)

We measure the linear viscoelasticity of sterically entangled and chemically cross-linked networks of actin filaments over more than five decades of frequency. The high-frequency response reveals rich dynamics unique to semiflexible polymers, including a previously unobserved relaxation due to rapid axial tension propagation. For high molecular weight, and for cross-linked gels, we obtain quantitative agreement with predicted shear moduli in both amplitude and frequency dependence.

DOI: [10.1103/PhysRevLett.96.138307](https://doi.org/10.1103/PhysRevLett.96.138307)

PACS numbers: 83.80.Lz, 82.70.Gg, 83.80.Rs, 87.16.Ka

The machinery that drives essential functions of cells such as locomotion and division is based on an elastic network of interconnected semiflexible protein filaments, collectively referred to as the cytoskeleton [1]. A major component of the cytoskeleton is the actin cortex, a dense meshwork of cross-linked actin filaments beneath the plasma membrane that is controlled by a host of accessory proteins. The physical construction of the cytoskeleton with its complex hierarchy of structural length scales enables the cell to produce large changes in physical properties by small chemical interventions, such as length- or crosslink-control or regulated attachments to other structures in the cell. The unique sensitivity of cytoskeletal networks stems in large part from the semiflexible character of its constituents, i.e., the fact that their thermal persistence length  $l_p$  [ $17\ \mu\text{m}$  for filamentous-actin (F-actin) [2]] is orders of magnitude larger than molecular scales ( $7\ \text{nm}$  filament diameter of actin [2]).

The mechanical and dynamical (rheological) properties of semiflexible polymers have been the focus of intense research in recent years. Apart from their biological role, these networks have proven to be unique polymeric materials in their own right. In contrast to flexible polymer networks, the shear modulus of a semiflexible polymer network can be varied over many orders of magnitude by small changes in cross-linking [3–6], and exhibits strong nonlinearities [3,5,7,8]. The dynamics of semiflexible solutions and gels have proven to be much richer than those of flexible polymers. Even for single filaments there are multiple distinct modes of relaxation that are qualitatively distinct from those of conventional polymers [7,9–11]. It has proven challenging, however, to quantitatively probe those dynamic regimes experimentally, because of the extensive bandwidth required.

Here, we have measured the dynamic shear modulus of F-actin solutions and cross-linked gels over a range of frequencies from 1 Hz to nearly 100 kHz. We find quantitative agreement with theory for the modulus at high frequencies, confirming the principal role of transverse thermal bending fluctuations in determining the network response [12,13]. Furthermore, we demonstrate an intermediate-frequency relaxation mode that is unique to

semiflexible polymers, and is due to rapid stress propagation along the filament backbone leading to a retraction of the chain ends. This effect has been predicted [13–16], but has not been observed previously.

We achieve a bandwidth of 100 kHz by using an optical microrheology technique based on laser-interferometric detection of thermal fluctuations of embedded probe particles [11,17]. We have here used two-particle microrheology, measuring the cross-correlated thermal motion of pairs of particles at well-defined separations. Correlations in displacements result from hydrodynamic and elastic interactions transmitted through the intervening material and report bulk viscoelasticity, virtually unaffected by the local particle environment [18,19]. In contrast, the shear moduli derived from one-particle microrheology in actin have been shown to differ from the bulk moduli measured with conventional rheometers [18,20].

Samples were prepared by mixing monomeric actin (G-actin) [21] with silica spheres of  $1.16\ \mu\text{m}$  diameter, which were larger than the average mesh size [22]  $\xi = 0.3/\sqrt{c_A}$ , with  $c_A$  the actin concentration (0.5 to 2 mg/ml) [23]. Embedded silica particles with diameters less than  $7\ \mu\text{m}$  did not settle under gravity during the course of the experiments. Polymerization was initiated by buffer change [21] and the sample was loaded into a glass chamber and equilibrated for 1 h at room temperature. Cross-linking was achieved by mixing G-actin (A) with biotinylated actin (B) (ratio  $r_{AB} = 50$ ) and neutravidin (N) ( $r_{AN} = 25$ ). Microrheology was performed using laser interferometry and quadrant-photodiode detection in an inverted microscope, providing subnanometer resolution at 100 kHz bandwidth [11,17]. Pairs of probe particles located at least  $20\ \mu\text{m}$  away from the sample chamber walls were illuminated by two weak ( $<5\ \text{mW}$ ) focused laser beams (wavelengths 1064 and 830 nm). The photodiode signals corresponding to the displacements of the two particles (labeled 1 and 2) from their respective detector-beam axes in the directions parallel ( $x$ ) and perpendicular ( $y$ ) to the line connecting them were digitized at 195 kHz after antialias filtering [17]. From the measured fluctuations  $x_{1,2}(t)$  and  $y_{1,2}(t)$  we calculated the parallel and perpendicular time-averaged cross-correlation functions,

$C_{\parallel}(\omega) = \int dt e^{i\omega t} \langle x_1(t)x_2(0) \rangle$  and  $C_{\perp}(\omega) = \int dt e^{i\omega t} \langle y_1(t)y_2(0) \rangle$ . For an isotropic and homogeneous medium, these two components completely characterize the full tensorial correlations. The fluctuation-dissipation theorem relates these correlation functions to the corresponding mutual displacement response functions [24],  $\alpha_{\parallel,\perp}(\omega) = \alpha'_{\parallel,\perp}(\omega) + i\alpha''_{\parallel,\perp}(\omega)$ :

$$C_{\parallel,\perp}(\omega) = (2k_B T/\omega)\alpha''_{\parallel,\perp}, \quad (1)$$

where  $k_B T$  is the thermal energy, and  $\alpha''_{\parallel,\perp}(\omega)$  refer to the imaginary parts of the complex response functions. The respective real parts  $\alpha'_{\parallel,\perp}(\omega)$  are computed from  $\alpha''_{\parallel,\perp}(\omega)$  by Kramers-Kronig integrals [11,24]. The connection between the complex response functions (corrected for the weak harmonic potentials created by the focused lasers [17]) and the complex shear modulus  $G^*(\omega)$  is given by a generalization of the Oseen tensor [18,19]:

$$\alpha_{\parallel} = 2\alpha_{\perp} = 1/[4\pi r_{12} G^*(\omega)]. \quad (2)$$

The complex modulus  $G^*(\omega)$  has real and imaginary parts,  $G'(\omega)$  and  $G''(\omega)$ , which are known as the storage and loss modulus, respectively. For a viscous liquid of viscosity  $\eta$ ,  $G^*(\omega) = -i\omega\eta$ , and these expressions reduce to the familiar Oseen tensor [25]. Equation (2) assumes an incompressible viscoelastic medium [11,26]. This assumption is validated by our data, showing consistent results for  $G^*(\omega)$  from the parallel and perpendicular displacement correlations. The shear moduli presented here are based on the less noisy parallel channel. For separation distances  $r_{12} = 3\text{--}20 \mu\text{m}$  there was no distance dependence of the moduli, consistent with the assumption that the material connecting the particles at these distances behaves as a bulk viscoelastic material [18,19].

Figures 1(a) and 1(b) show the storage and loss moduli,  $G'(\omega)$  and  $G''(\omega)$ , of a 1 mg/ml solution of F-actin without and with cross-linking. The non-cross-linked solution has a low-frequency modulus of around 0.2 Pa, similar to values measured previously with conventional rheology [4] and microrheology [6,11,20]. The storage modulus shows no discernible elastic plateau over the frequency range studied here. After cross-linking, the storage modulus develops a plateau of around 46 Pa, while the loss modulus is slightly increased at intermediate frequencies and scales with frequency as  $G''(\omega) \sim \omega^{3/4}$ . Data at high frequencies can be quantitatively compared with theory. Theoretical models of the viscoelastic response of semiflexible polymer networks [12,13] predict that the shear modulus at high frequencies is entirely controlled by the relaxation of individual polymer chains. When a polymer network is sheared, the thermally undulating filaments are either compressed or stretched, depending on their orientation with respect to the shear direction. Since the filaments are practically inextensible along their contour, the chain conformations rethermalize by a redistribution of their bending modes, leading to a characteristic scaling of the

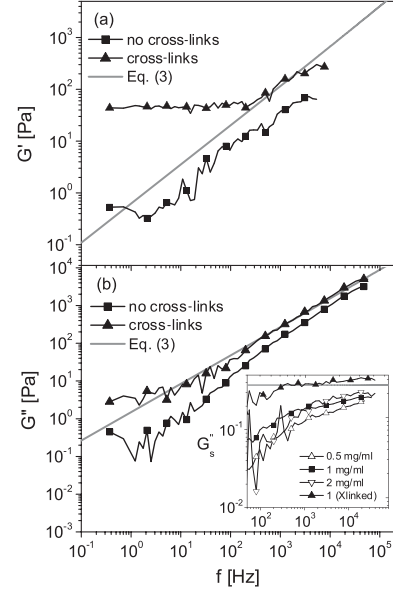


FIG. 1. (a) Storage modulus  $G'(\omega)$  and (b) (absolute) loss modulus  $G''(\omega)$  of 1 mg/ml solutions of F-actin filaments without (squares) and with (triangles) cross-linking plotted against frequency  $f = \omega/2\pi$ . Solid lines: theory, Eq. (3). Inset: scaled loss modulus  $G''_s(\omega) = -[G''(\omega) + i\omega\eta]/(c_A\omega^{3/4})$ .

polymer contribution to the shear modulus as  $G^*(\omega) \propto \omega^{3/4}$  [12,13]:

$$G^*(\omega) \approx \frac{1}{15}\rho\kappa l_p (-2i\zeta/\kappa)^{3/4} \omega^{3/4} - i\omega\eta. \quad (3)$$

The linear (viscous) term in frequency dominates at high frequencies (above the range of our experiments). In Eq. (3), the density (length/volume) of filaments  $\rho = c_A \times 3.8 \times 10^{13} \text{ m}^{-2}$ , the bending stiffness  $\kappa = l_p/k_B T$ , and the lateral drag coefficient per unit length  $\zeta \approx 0.0023 \text{ N s/m}^2$ , are all known [12,13]. Thus, the solid lines in Figs. 1(a) and 1(b) represent the prediction of Eq. (3) with no adjustable parameters. The measured loss modulus  $G''(\omega)$  for entangled actin approaches the theoretical prediction only at the highest frequencies probed, while upon cross-linking with practically irreversible biotin-neutravidin bonds,  $G''(\omega)$  agrees with Eq. (3) over the whole experimental frequency range. The storage modulus  $G'(\omega)$  for entangled actin also remains below the theoretical curve over the whole frequency range probed, while cross-linking leads to better agreement with Eq. (3) above the plateau. (The elastic moduli are cut off at about 10 kHz, due to the high-frequency limit of the Kramers-Kronig integral.) The plateau value of 46 Pa at low frequencies is consistent with theory [3,12] for an average distance between cross-links of about  $1.8 \mu\text{m}$ .

In a regime where the modulus is dominated by single-filament dynamics, it should be linear in actin concentration  $c_A$ . By contrast, collective phenomena (e.g., entanglement) will result in a stronger dependence. The inset of Fig. 1(b) demonstrates the linear concentration dependence of the polymer contribution to the loss modulus, as ex-

pected from Eq. (3). From the lack of collapse of the non-crosslinked data, however, there seems to be a slight increase of the scaled modulus with actin concentration. This may reflect a concentration-dependent filament length distribution.

Naïvely one would expect that entangled and cross-linked semiflexible polymer networks are indistinguishable at frequencies above the elastic plateau. The fact that the shear moduli for entangled solutions of actin are below both the cross-linked and the theoretically predicted modulus implies an additional mechanism for relaxation of stress that disappears with cross-linking. The deviation from Eq. (3) is emphasized in the inset of Fig. 1(b), where the loss moduli are multiplied by  $\omega^{-3/4}$ . This inset also shows that the increased relaxation at intermediate frequencies is present for a range of actin concentrations. It has recently been suggested [13–16] that, in the case of semiflexible polymers of finite length, rapid tension propagation along the filament backbone leads to an additional relaxation of network stress by the retraction or extension of filament ends. Experimental proof of this mechanism has been lacking so far. The data in Fig. 1 provide one test for this mechanism. Cross-linking should prevent filament end retraction, and indeed we find quantitative agreement with high molecular weight theory upon cross-linking [Eq. (3), solid lines in Fig. 1].

We further test for this relaxation mechanism by examining the polymer length dependence, which should be strong since the time it takes for tension to propagate along a filament of length  $L$  increases rapidly with length as  $t \sim L^8$  [13–16]. For shorter filaments the transition to the  $\omega^{3/4}$  regime should occur at higher frequencies, and the network should be softer at lower frequencies. To control average filament length we added the physiological capping protein gelsolin [27]. G-actin was polymerized at a fixed concentration of 1 mg/ml in the presence of gelsolin at actin/gelsolin molar ratios  $r_{AG} = 370$ –6290. Assuming random capping [27], we estimate average lengths between 1 and 17  $\mu\text{m}$ . Figs. 2(a) and 2(b) show that the storage and loss moduli indeed decrease as the filament length is reduced. The slope of  $G''(\omega)$  (corrected for the solvent contribution) increasingly approaches 1, which is also consistent with a larger contribution of chain-end retraction to the stress relaxation. At present, there is no theory that accounts for the longitudinal relaxation while spanning dilute solutions and strongly entangled regimes. The lines in Figs. 2(a) and 2(b) are the predictions of Refs. [13,16] for dilute solutions of short chains (3  $\mu\text{m}$ , bottom) and entangled solutions of long chains (17  $\mu\text{m}$ , middle). This theory with chain-end corrections, although it does not take into account the exponential length distribution of actin filaments [27], qualitatively captures the trend towards lower shear moduli for shorter chains. The observed change in slope of  $G''(\omega)$  to values higher than 3/4 is also consistent with the theoretical predictions.

The shear moduli reported here were all obtained from thermal fluctuations of embedded probe particles using

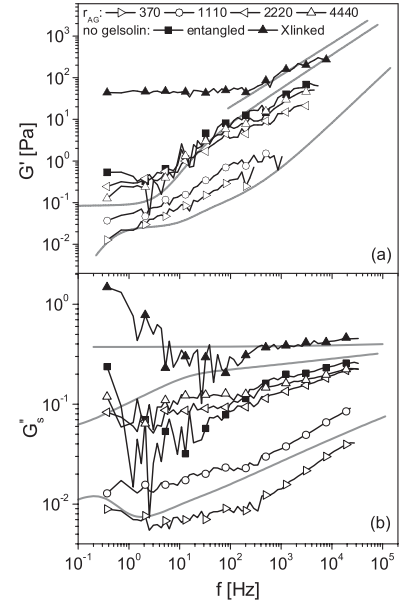


FIG. 2. Filament length dependence of the storage modulus  $G'(\omega)$  (a) and scaled loss modulus  $G''_s$  (b) of a 1.0 mg/ml solution of F-actin filaments shortened with different amounts of gelsolin as indicated. Solid symbols: unshortened actin (see Fig. 1). Lines: high molecular weight theory, Eq. (3) (top), finite length theory with average lengths 17  $\mu\text{m}$  (middle) and 3  $\mu\text{m}$  (bottom).

Eq. (2), which assumes an incompressible homogeneous medium [11,26]. Experimentally, the importance of compressibility can be tested by considering the (real part of the) ratio of the perpendicular and parallel cross-correlated particle displacements [19]:

$$[\alpha_{\perp}/\alpha_{\parallel}]' = \frac{3 - 4\sigma}{4(1 - \sigma)}, \quad (4)$$

which has physical bounds of 1/2 and 7/8, since the Poisson ratio  $\sigma$  is bounded by 1/2 and  $-1$ , where the former corresponds to an incompressible medium [11,26]. Figure 3 shows ratios  $[\alpha_{\perp}/\alpha_{\parallel}]'$  measured for three particle distances  $r_{12}$  in an entangled actin network. The ratio  $[\alpha_{\perp}/\alpha_{\parallel}]'$  is indeed close to 1/2, consistent with a strong viscous coupling of the actin network to the solvent and in support of the incompressibility assumption. The deviations apparent at high frequencies are quantitatively consistent with fluid inertial effects [28]. At low frequencies we are unable to demonstrate or exclude compressibility because of noise limitations, which are particularly pronounced in the perpendicular channel.

We have measured the complex shear modulus  $G^*(\omega)$  of F-actin solutions and gels over a wide frequency range. We show that at high frequencies the response is dominated by single-filament bending fluctuations and is in quantitative agreement with theory [12,13]. Further, we demonstrate a dynamic mode that is unique to (non-cross-linked) semiflexible polymers, which is due to rapid axial stress relaxation through free filament ends. Both relaxation modes are

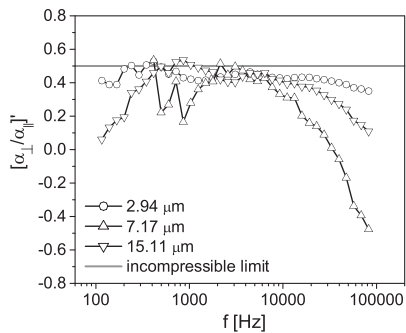


FIG. 3. Real part of the ratio of perpendicular to parallel response functions  $[\alpha_{\perp}/\alpha_{\parallel}]$  for a pair of  $1.16 \mu\text{m}$  beads in a  $1.0 \text{ mg/ml}$  actin solution at distances  $r_{12}$  as indicated.

only apparent at high frequencies which have not previously been accessible. Laser-based particle trapping and tracking methods such as those presented here open an extended view on complex polymer dynamics, which is very relevant for biological systems with their inherently broad distribution of characteristic time scales. Important future challenges include the extension of the high-frequency microrheology technique to include active driving of the particles and the study of the out-of-equilibrium properties of biological systems.

We thank A. Levine, D. Head, D. C. Morse, M. Pasquali, and K. M. Addas for helpful discussions, F. Gittes, J. Kwiecinska, and M. Buchanan for software, K. C. Vermeulen for actin, and P. A. Janmey for gelsolin. This work was supported by the Foundation for Fundamental Research on Matter (FOM) and by a European Marie Curie Fellowship (FP6-2002-Mobility-6B, Contract No. 8526).

\*Present address: Division of Engineering and Applied Sciences, Harvard University, Cambridge, MA, USA.

†Present address: III. Physikalisches Institut, Fakultät für Physik, Georg-August-Universität, Göttingen, Germany. Email address: cfs@physik3.gwdg.de

- [1] B. Alberts, D. Bray, J. Lewis, M. Raff, K. Roberts, and J. D. Watson, *Molecular Biology of the Cell* (Garland publishing, New York, 1994).
- [2] F. Gittes, B. Mickey, J. Nettleton, and J. Howard, *J. Cell Biol.* **120**, 923 (1993).
- [3] F. C. MacKintosh, J. Käs, and P. A. Janmey, *Phys. Rev. Lett.* **75**, 4425 (1995).
- [4] J. Y. Xu, W. H. Schwarz, J. A. Käs, T. P. Stossel, P. A. Janmey, and T. D. Pollard, *Biophys. J.* **74**, 2731 (1998).
- [5] M. L. Gardel, J. H. Shin, F. C. MacKintosh, L. Mahavedan, P. Matsudaira, and D. A. Weitz, *Science* **304**, 1301 (2004); M. L. Gardel, J. H. Shin, F. C. MacKintosh, L. Mahavedan, P. A. Matsudaira, and D. A. Weitz, *Phys. Rev. Lett.* **93**, 188102 (2004).
- [6] A. Palmer, J. Xu, and D. Wirtz, *Rheol. Acta* **37**, 97 (1998).
- [7] P. A. Janmey, S. Hvidt, J. Kas, D. Lerche, A. Maggs, E. Sackmann, M. Schliwa, and T. P. Stossel, *J. Biol. Chem.* **269**, 32503 (1994).
- [8] C. Storm, J. J. Pastore, F. C. MacKintosh, T. C. Lubensky, and P. A. Janmey, *Nature (London)* **435**, 191 (2005).
- [9] F. Amblard, A. C. Maggs, B. Yurke, A. N. Pargellis, and S. Leibler, *Phys. Rev. Lett.* **77**, 4470 (1996).
- [10] H. Isambert and A. C. Maggs, *Macromolecules* **29**, 1036 (1996).
- [11] F. Gittes, B. Schnurr, P. D. Olmsted, F. C. MacKintosh, and C. F. Schmidt, *Phys. Rev. Lett.* **79**, 3286 (1997); B. Schnurr, F. Gittes, F. C. MacKintosh, and C. F. Schmidt, *Macromolecules* **30**, 7781 (1997).
- [12] F. Gittes and F. C. MacKintosh, *Phys. Rev. E* **58**, R1241 (1998).
- [13] D. C. Morse, *Phys. Rev. E* **58**, R1237 (1998); *Macromolecules* **31**, 7044 (1998).
- [14] R. Everaers, F. Juelicher, A. Ajdari, and A. C. Maggs, *Phys. Rev. Lett.* **82**, 3717 (1999).
- [15] M. Pasquali, V. Shankar, and D. C. Morse, *Phys. Rev. E* **64**, 020802 (2001).
- [16] V. Shankar, M. Pasquali, and D. C. Morse, *J. Rheol. (N.Y.)* **46**, 1111 (2002).
- [17] M. Atakhorrami, J. I. Sulkowska, K. M. Addas, G. H. Koenderink, J. X. Tang, A. J. Levine, F. C. MacKintosh, and C. F. Schmidt *Phys. Rev. E* (to be published).
- [18] J. C. Crocker, M. T. Valentine, E. R. Weeks, T. Gisler, P. D. Kaplan, A. G. Yodh, and D. A. Weitz, *Phys. Rev. Lett.* **85**, 888 (2000).
- [19] A. J. Levine and T. C. Lubensky, *Phys. Rev. Lett.* **85**, 1774 (2000); *Phys. Rev. E* **65**, 011501 (2002).
- [20] M. L. Gardel, M. T. Valentine, J. C. Crocker, A. R. Bausch, and D. A. Weitz, *Phys. Rev. Lett.* **91**, 158302 (2003).
- [21] J. D. Pardee and J. A. Spudich, in *Structural and Contractile Proteins Part B: The Contractile Apparatus and the Cytoskeleton*, edited by D. W. Frederiksen and L. W. Cunningham (Academic Press, San Diego, 1982), p. 164. Actin was purified from rabbit skeletal muscle and stored in G-buffer (2 mM Tris, 0.2 mM  $\text{CaCl}_2$ , 0.2 mM  $\text{Na}_2\text{ATP}$ , 0.5 mM  $\text{NaN}_3$ , 2 mM DTT, pH 8.0) at  $-80^\circ\text{C}$ . Thawed actin was polymerized by adding  $10\times$  F-buffer to a final concentration of 2 mM HEPES, 2 mM  $\text{MgCl}_2$ , 50 mM KCl, 1 mM  $\text{Na}_2\text{ATP}$ , 1 mM EGTA, pH 7.5.
- [22] C. F. Schmidt, M. Bärmann, G. Isenberg, and E. Sackmann, *Macromolecules* **22**, 3638 (1989).
- [23] The actin concentration was determined from the absorbance at 280 nm (extinction coefficient  $0.65 \text{ cm}^{-1} \text{ ml mg}^{-1}$ ) and a Bradford assay.
- [24] L. D. Landau and E. M. Lifshitz, *Mechanics*, Course of Theoretical Physics Vol. 1 (Elsevier, Oxford, 1960).
- [25] C. W. Oseen, *Neuere Methoden und Ergebnisse in der Hydrodynamik* (Akademische Verlagsgesellschaft, Leipzig, 1927).
- [26] A. J. Levine and T. C. Lubensky, *Phys. Rev. E* **63**, 041510 (2001).
- [27] S. Burlacu, P. A. Janmey, and J. Borejdo, *Am. J. Physiol.* **262**, C569 (1992).
- [28] M. Atakhorrami, G. H. Koenderink, C. F. Schmidt, and F. C. MacKintosh, *Phys. Rev. Lett.* **95**, 208302 (2005); T. B. Liverpool and F. C. MacKintosh, *ibid.* **95**, 208303 (2005).